EPJ Web of Conferences **38**, 02001 (2012)
DOI: 10.1051/epjconf/20123802001


# Covariant density functional theory and applications in nuclear physics and r-process

P. W. Zhao[1], L. L. Li[2], Z. P. Li[3], Z. M. Niu[4], P. Ring[1,5], J. M. Yao[3], S. G. Zhou[6,7], and J. Meng[1,8,9,a]

[1] State Key Laboratory of Nuclear Physics and Technology, School of Physics, Peking University, Beijing 100871, China
[2] Beijing Institute of Applied Physics and Computational Mathematics, Beijing 100094, China
[3] School of Physical Science and Technology, Southwest University, Chongqing 400715, China
[4] School of Physics and Material Science, Anhui University, Hefei 230039, China
[5] Physikdepartment, Technische Universität München, 85748 Garching, Germany
[6] State Key Laboratory of Theoretical Physics, Institute of Theoretical Physics, Chinese Academy of Sciences, Beijing 100190, China
[7] Center of Theoretical Nuclear Physics, National Laboratory of Heavy Ion Accelerator, Lanzhou 730000, China
[8] School of Physics and Nuclear Energy Engineering, Beihang University, Beijing 100191, China
[9] Department of Physics, University of Stellenbosch, Stellenbosch, South Africa

**Abstract.** The covariant density functional theory (CDFT) with a few number of parameters allows a very successful description of the properties of nuclei all over the nuclear chart. The recent progress on the application of the CDFT as well as its extensions for a series of interesting and hot topics in nuclear structure and nuclear astrophysics are summarized. In particular, the newly proposed point-coupling parametrization PC-PK1 and the application of the CDFT to the single particle level of the radioactive neutron-rich doubly magic nucleus $^{132}$Sn, the deformed halo in nuclei, and the $\beta$ decay life-time of neutron rich nuclei are discussed in details.

## 1 Introduction

In the past decades, the radioactive ion beams (RIB) have extended our knowledge of nuclear physics from the stable nuclei to the unstable nuclei far away from the stability line — the so-called "exotic nuclei". The investigation of exotic nuclei has attracted world-wide attention due to their large isospin values and intriguing properties, such as the halo phenomenon. Furthermore, the properties of exotic nuclei play essential roles in understanding the nucleosynthesis in the rapid neutron-capture process (*r*-process).

The density functional theory (DFT) is well known for its numerous applications to description of nuclear ground and excited states. In particular, the covariant version of DFT takes the Lorentz symmetry into account in a self-consistent way. During the past years, the covariant DFT has received wide attention due to its successful description of lots of nuclear phenomena [1,2]. In practical applications, there are two widely used models in the covariant density functional theory (CDFT) framework: the relativistic Hartree (RH) and relativistic Hartree-Fock (RHF) models. The former one is usually known as the relativistic mean field (RMF) model.

There exist a number of attractive features in the CDFT. The most obvious one is the natural inclusion of the spin degree of freedom and the resulting spin-orbit potential that emerges automatically with the empirical strength in a covariant way. The relativistic effects are responsible for the existence of approximate pseudospin symmetry [3–6] in the nuclear single-particle spectra and spin symmetry in the anti-nucleon spectra [7]. The representations with large scalar and vector fields in nuclei, of the order of a few hundred MeV, provide more efficient descriptions than non-relativistic approaches that hide these scales. Moreover, it is of particular importance that the CDFT includes nuclear magnetism [8], i.e., a consistent description of currents and time-odd fields, which plays an important role in the nuclear rotations [9–12].

In the conference, we presented the recent progress in the application of the CDFT as well as its extensions by the group in Beijing for a series of interesting and hot topics in nuclear structure and nuclear astrophysics including

- a newly developed point-coupling parametrization PC-PK1, which particularly improves the description for isospin dependence of the binding energy [13];
- a description for the radioactive neutron-rich doubly magic nucleus $^{132}$Sn, in particular, for the neutron single-particle spectrum [14];
- a deformed relativistic Hartree-Bogoliubov model in continuum in a Woods-Saxon basis, which aims at a proper description of exotic nuclei, in particular, deformed halo nuclei [15];
- a study of $\beta$ decay life-time of neutron rich nuclei based on self-consistent covariant quasiparticle random phase approximation [16].

In this contribution, these topics will be discussed in details.

## 2 PC-PK1 parametrization

The parametrization of PC-PK1 is determined by a multiparameter fitting to both the binding energies for 60 se-

[a] e-mail: mengj@pku.edu.cn

lected spherical nuclei and charge radii for 17 ones with the Levenberg-Marquardt method. Meanwhile, the empirical pairing gaps for 6 nuclei obtained with the five-point formula are also employed to constrain the pairing strengths. With the experimental observables and the calculated values, the ensemble of parameters can be obtained by minimizing the square deviation. More details for the fitting procedure and coupling constants of the parametrization PC-PK1 can be found in Ref. [13].

As shown in Ref. [13], binding energies and quadrupole deformations of the ground states of Yb and U isotopes are investigated. In the upper panels of figure 1, the deviations of the calculated binding energies with PC-PK1 [13], DD-PC1 [17], and PC-F1 [18] from the data [19] are shown. When the rotational corrections are not taken into account, a systematic underestimation of the binding energies around 3 MeV for both Yb and U isotopes is found for PC-PK1. For PC-F1, however, the differences between the calculated and the observed binding energies decrease monotonically with the neutron numbers. Since almost all the isotopes shown in figure 1 are employed to adjust the parameters of DD-PC1, its predictions are in good agreement with the data (within 1 MeV).

After taking into account the rotational correction energies with the cranking approximation [20], the calculated results with PC-PK1 reproduce the data quite well (within 1 MeV) for both Yb and U isotopes, while the differences between the corrected binding energies given by PC-F1 and data are still large. Since DD-PC1 is adjusted to the binding energies of well-deformed nuclei, the rotational correction energy is not considered in the corresponding calculations.

The calculated ground state deformations are shown in the lower panels of figure 1 in comparison with the data available [21]. It is found that PC-PK1 provides also good performance in the description of deformations as well as their corresponding evolutions with neutron number for both Yb and U isotopes.

For the nuclear matter, as in Ref. [13], the saturation properties and the equation of states (EOS) were investigated in the CDFT with PC-PK1 and the results were compared with the corresponding empirical values as well as the predictions with other effective interactions. Here, we mainly focus on the nuclear matter incompressibility $K_0$ and the asymmetry term of nuclear incompressibility $K_\tau$.

The study of the nuclear matter incompressibility $K_0$ continues to be a hot topic in both the theoretical and experimental fields, since its value is one of the most fundamental quantity in determining the EOS of nuclear matter. The nuclear matter incompressibility $K_0$ cannot be directly measured, while the energy of isoscalar giant monopole resonance (ISGMR) which is related to the finite nucleus incompressibility $K_A$ can be determined experimentally. Moreover, the finite nucleus incompressibility $K_A$ can be expressed in terms of [22]

$$K_A = K_0 + K_{\rm surf} A^{-1/3} + K_\tau[(N-Z)/A]^2 + K_{\rm Coul} Z^2 A^{-4/3}, \quad (1)$$

where $K_\tau$ is the asymmetry term which is associated with the neutron excess and is very crucial in the study of neutron stars.

In figure 2, the values of nuclear matter incompressibility $K_0$ and the asymmetry term of nuclear incompressibility $K_\tau$ for the 25 parameter sets in both the relativistic and non-relativistic density functional theories are shown. One could see that the predicted results with PC-PK1 are in very good agreement with the corresponding experiment constraints (see Ref. [23] and references therein).

## 3 Neutron single-particle spectrum in $^{132}$Sn

The magic numbers is one of the most fundamental ingredients for understanding the nature of atomic nuclei. Recently, by using the $^{132}$Sn(d, p)$^{133}$Sn reaction, the experiment performed at Oak Ridge National Laboratory revealed for the first time that the spectroscopic factors of the neutron single-particle states $3p_{1/2}, 3p_{3/2}, 2f_{5/2}$, and $2f_{7/2}$ outside the $N = 82$ core are consistent with $S \approx 1$ [25]. This is one of the critical pieces of evidence to conclude that $^{132}$Sn is a perfectly radioactive doubly magic nuclei, even better than the stable $^{208}$Pb.

In Ref. [14], the CDFT is applied to investigate the properties of the radioactive neutron-rich doubly magic nucleus $^{132}$Sn and the corresponding isotopes and isotones.

In figure 3, we show the neutron-effective single-particle energies (SPE) with respect to the orbital $2f_{7/2}$ in $^{132}$Sn calculated by the RMF theory with PC-PK1 [13], NL3* [26], DD-ME2 [27], PK1 [28], and PKDD [28] in comparison with the data [25] and results calculated by the Skyrme-Hartree-Fock theory with the typical effective interactions SkP [29], SkM* [30], BSK17 [31], SLy4 [32], and SIII [33]. In the present mean-field level, it is clearly shown that the overall structure of the neutron-effective SPE for such a neutron-rich doubly magic nucleus can be well reproduced in the relativistic framework, where both the spin-orbit and orbit-orbit potentials are described in a self consistent way. In contrast, the nonrelativistic results overestimate nearly twice the single-particle energy spacing between the orbitals $3p_{3/2}$ and $2f_{7/2}$, where the reduction of the orbit-orbit potential plays the most important role.

Furthermore, one can extract the Nilsson spin-orbit parameter $C$ and orbit-orbit parameter $D$ by fitting to the single-particle energies. As discussed in Ref. [14], the RMF results agree quite well with the extracted Nilsson spin-orbit parameter $C$ and orbit-orbit parameter $D$ from experimental SPE of $^{132}$Sn, but remarkably differ from the traditional Nilsson parameters.

## 4 Deformed halo in nuclei

Halo is one of the most interesting exotic nuclear phenomena. There are many new features in the halo nuclei because of the extremely weakly binding properties. To give a proper theoretical description of the halo phenomena, it is crucial to treat properly the coupling between bound states and the continuum due to pairing correlations by either the finite range or the zero range pairing forces [34] and the very extended spatial density distributions. This can be achieved by solving, in the coordinate ($r$) space or equivalent basis, the non-relativistic Hartree-Fock-Bogoliubov (HFB) [29,35] or the relativistic Hartree Bogoliubov (RHB) [36–39] equations .

For the spherical nuclei, with the relativistic continuum Hartree Bogoliubov (RCHB) theory [40] in coordinate space, the halo in nucleus $^{11}$Li has been reproduced

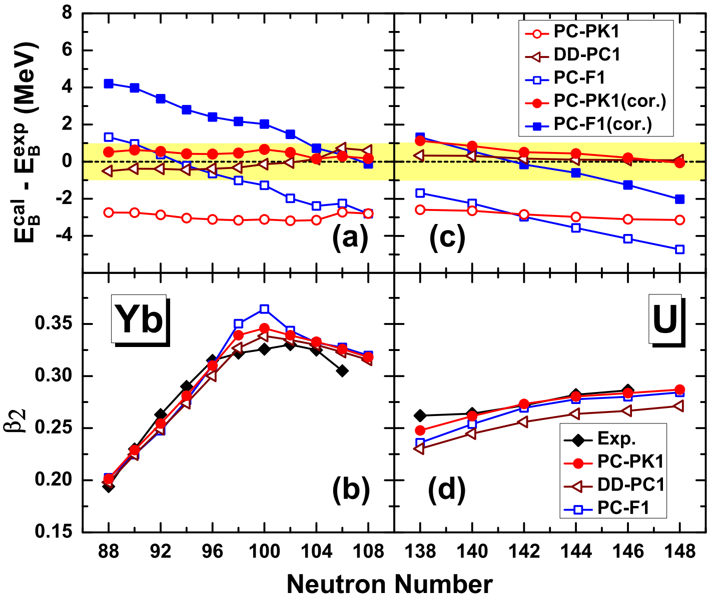


**Fig. 1.** Deviations of the calculated binding energies from the data [19] for Yb and U isotopes obtained by PC-PK1 [13], DD-PC1 [17], and PC-F1 [18] (upper panels) as well as the corresponding calculated ground state deformations in comparison with data [21] (lower panels). The filled circles and squares in the upper panels correspond to the rotational corrected values given by PC-PK1 and PC-F1, respectively. Taken from Ref. [13].

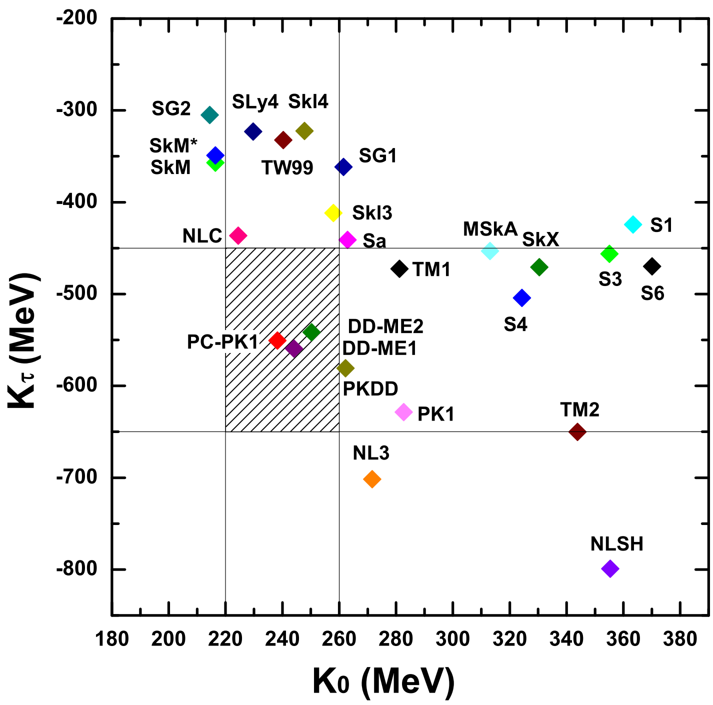


**Fig. 2.** Correlations between the nuclear matter incompressibility $K_0$ and the asymmetry term of nuclear incompressibility $K_\tau$ for the 25 parameter sets in both the relativistic and non-relativistic density functional theories. Constraints for $K_0$ from the giant monopole resonance (GMR) data on $^{208}$Pb and $^{90}$Zr and for $K_\tau$ from the isotopic dependence of the GMR in the even-A Sn isotopes [23] are represented by the shadow area. The calculated results are taken from Ref. [24] except for that with PC-PK1.

quite well [36] and the giant halos in light and medium-heavy nuclei was predicted in Refs. [39,41,42]. Moreover, the RCHB theory has been generalized to treat the odd particle system [43].

For deformed nuclei, on the other hand, the Woods-Saxon basis has been proposed in Ref. [44] to solve the deformed RHB equation with proper treatment for the asymptotic behavior of nuclear densities at large $r$. Over the past years, lots of efforts have been made to develop a deformed relativistic Hartree theory [45] and a deformed relativistic Hartree Bogoliubov theory in continuum (the DefRHBC theory) [46,15,47]. Recently, the DefRHBC theory has been further extended to treat the odd-$A$ or odd-odd nuclei by including the blocking effect due to the odd nucleon(s) [48] and the density-dependent meson-nucleon couplings version [49].

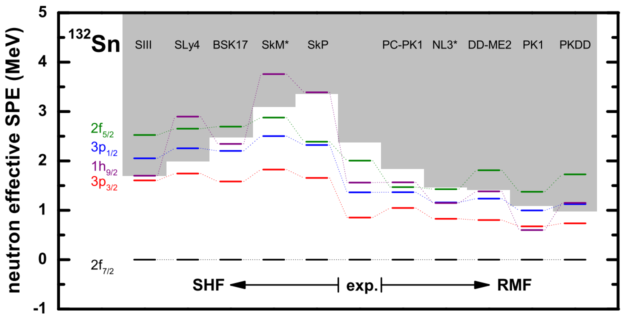


**Fig. 3.** Neutron-effective single-particle energies with respect to the orbital $2f_{7/2}$ in $^{132}$Sn calculated by the RMF theory with effective interactions PC-PK1 [13], NL3* [26], DD-ME2 [27], PK1 [28], and PKDD [28]. The experimental data [25] and the results calculated by the Skyrme-Hartree-Fock theory with SkP [29], SkM* [30], BSK17 [31], SLy4 [32], and SIII [33] are also shown for comparison. The shaded areas indicate the area beyond the neutron threshold. Taken from Ref. [14].

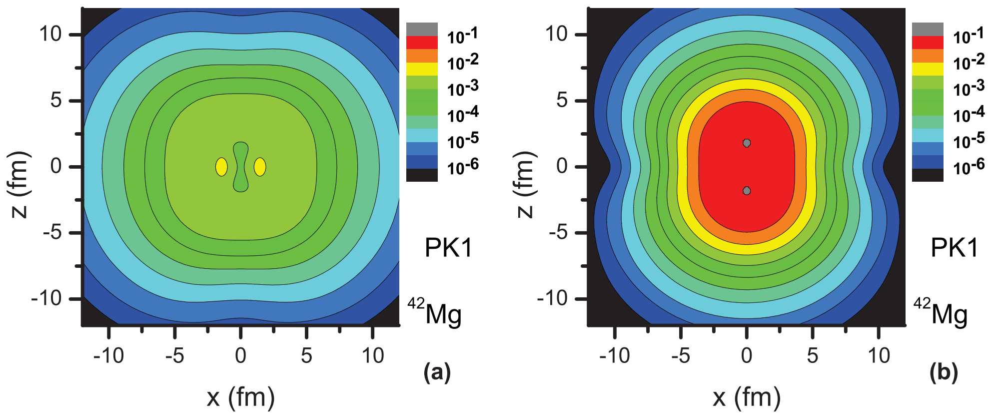


**Fig. 4.** Density distributions for the neutron halo (a) and the neutron core (b) for the ground state of $^{42}$Mg. Here, the $z$ axis is the symmetry axis. Taken from Ref. [47].

The halo phenomenon in deformed nuclei has been investigated with the DefRHBC theory in Refs. [15,47]. In some deformed neutron-rich nuclei, e.g., $^{42,44}$Mg, a decoupling of the halo orbitals from the deformation of the core has been predicted. Here, we present and discuss in details the results from the DefRHBC theory for the deformed neutron-rich and weakly bound nucleus $^{42}$Mg [15,47].

Magnesium isotopes have been studied extensively in Refs. [15,47] with the deformed relativistic Hartree Bogoliubov theory in continuum and the parameter sets NL3 [50] and PK1 [28]. In the calculations with the PK1, $^{42}$Mg is predicted as the last bound nucleus in Mg isotopes [47].

As discussed in Ref. [47], the ground state of $^{42}$Mg is well deformed with a quadrupole deformation $\beta \approx 0.41$, and a very small two neutron separation energy $S_{2n} \approx 0.22$ MeV. In the tail part, the neutron density extends more along the direction perpendicular to the symmetry axis. In figure 4, the density distribution is decomposed into the contributions from the oblate "halo" and the prolate "core", respectively. The density distribution of this weakly bound nucleus has a very long tail in the direction perpendicular to the symmetry axis. As explained in Ref. [47], this indicates that the prolate nucleus $^{42}$Mg has an oblate halo and there is a decoupling between the deformations of the core and the halo.

In figure 5, the single particle spectrum around the Fermi level for the ground state of $^{42}$Mg is presented together with the good quantum numbers of each single particle state. Here, the occupation probabilities $v^2$ in the canonical basis which are of the BCS-form [51] are given by the length of the horizontal lines. The levels near the threshold are labeled by the number $i$ according to their energies. Meanwhile, their good quantum number $\Omega^\pi$ and the main spherical components are given at the right hand side.

The neutron Fermi level locates in the $pf$ shell and most of the single particle levels nearby have negative parities. Since the chemical potential $\lambda_n$ is close to the continuum, orbitals above the threshold have noticeable occupations due to the pairing correlations. The single neutron levels of $^{42}$Mg can be divided into two parts, the deeply bound levels ($\varepsilon_{\text{can}} < -2$ MeV) corresponding to the "core", and the remaining weakly bound levels close to the threshold ($\varepsilon_{\text{can}} > -0.3$ MeV) and the continuum corresponding to the "halo".

As explained in Refs. [15,47], the shape of the halo results from the intrinsic structure of the weakly bound and continuum orbitals. By examining the neutron density distribution, we could learn that the halo in $^{42}$Mg is mainly formed by level 4 and level 5 composed of $p$ and $f$ components. Note that the angular distribution of $|Y_{10}(\theta,\phi)|^2 \propto \cos^2\theta$ with a projection of the orbital angular momentum on symmetry axis $\Lambda = 0$ is prolate and that of $|Y_{1\pm1}(\theta,\phi)|^2 \propto \sin^2\theta$ with $\Lambda = 1$ is oblate. It turns out that the $\Lambda = 1$ component dominates in level 4 ($\Omega^\pi = 1/2^-$) and is the sole component in level 5. Therefore, the shape of the halo in $^{42}$Mg is oblate and decouples from the corresponding prolate core.

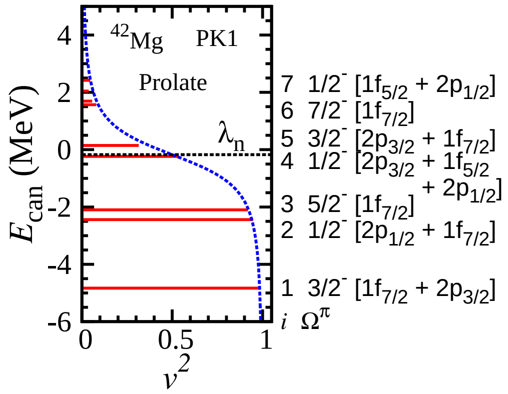


**Fig. 5.** Single neutron levels of ground state of $^{42}$Mg in the canonical basis as a function of the occupation probability $v^2$. The blue dashed line corresponds to the BCS-formula with an average pairing gap. Taken from Ref. [47].

For odd particle system, the formation and the size of a halo depend strongly on the interplay among the odd-even effects, continuum and pairing effects, deformation effects, etc. The work on this topic is still in progress [52].

## 5 Beta decay of neutron rich nuclei

Nuclear $\beta$ decay plays an important role not only in nuclear physics, but also in astrophysics and particle physics. With the development of radioactive ion beam facilities, the measurements of nuclear $\beta$ decay half-lives have achieved great progress in recent years, especially for nuclei with neutron numbers near $N = 50$ and $N = 82$ shell closures [19,53,54]. Recently, $\beta$ decay half-lives of very neutron-rich nuclei from Kr to Tc isotopes with neutron number between $N = 50$ and $N = 82$ have been measured [55].

Since majority of neutron-rich nuclei relevant to the *r*-process are still out of the reach of experimental capabilities, theoretical predictions are mandatory for the *r*-process calculations. In the framework of CDFT, the quasiparticle random phase approximation (QRPA) was combined with the RHB model [56] and was employed to calculate the $\beta$ decay half-lives of neutron-rich nuclei in the $N = 50$ and $N = 82$ regions [57,58].

Recently, a fully self-consistent proton-neutron QRPA based on the relativistic Hartree-Fock-Bogoliubov (RHFB) model is established [16]. With an isospin-dependent proton-neutron pairing interaction, the RHFB+QRPA approach is employed to calculate the decay half-lives of neutron rich nuclei with $20 \leq Z \leq 50$, covering the whole r-process path from $N = 50$ to $N = 82$. It is found that the RHFB+QRPA model well reproduces the experimental decay half-lives for neutron-rich nuclei, especially for the nuclei with calculated half-lives less than one second. The work on this topic is still in progress [16].

## 6 Summary

In summary, the recent progress in the application of the CDFT as well as its extensions by the group in Beijing for a series of interesting and hot topics in nuclear structure and nuclear astrophysics are summarized. In particular, the newly proposed point-coupling parametrization PC-PK1 and the application of the CDFT to the single particle levels of the radioactive neutron-rich doubly magic nucleus $^{132}$Sn, the deformed halo in nuclei, and the $\beta$ decay life-time of neutron rich nuclei are discussed in details. It is found that PC-PK1 can provide very good descriptions for not only the finite nuclei but also the nuclear matter. Investigations have also been applied to the single-particle spectrum of the neutron-rich doubly magic nucleus $^{132}$Sn. It is found that the RMF results agree quite well with the experimental single-particle spectrum in $^{132}$Sn as well as the Nilsson spin-orbit parameter $C$ and orbit-orbit parameter $D$ thus extracted, but remarkably differ from the traditional Nilsson parameters. Moreover, the development of a deformed relativistic Hartree-Bogoliubov theory in continuum and the study of neutron halo in deformed nuclei $^{42}$Mg is presented. Pronounced deformed neutron halos and a decoupling between the shapes of the core and the halo were predicted. Finally, a fully self-consistent proton-neutron QRPA based on the RHFB model and its applications to the $\beta$ decay life-time of neutron rich nuclei are briefly reported.

## Acknowledgments

This work was supported in part by the Major State 973 Program of China (Grant No 2013CB834400), the Natural Science Foundation of China (Grants No. 10875157, No. 10979066, No. 10975007, No. 10975100, No. 10975008, No. 11005069, No.11175002, No.11175252, No.11105005, No. 11105111, No. 11105110, No. 11121403, and No. 11120101005), the Research Fund for the Doctoral Program of Higher Education No.20110001110087, Fundamental Research Funds for the Central Universities (Grant No. XDJK2010B007 and No. XDJK2011B002), and Southwest University Initial Research Foundation Grants to Doctors (No. SWU109011 and No. SWU110039), and Knowledge Innovation Project of CAS (KJCX2-EW-N01 and KJCX2-YW-N32). Part of the results described in this contribution were obtained on the ScGrid of Supercomputing Center, Computer Network Information Center of Chinese Academy of Sciences.

## References

1. J. Meng, H. Toki, S. Zhou, S. Zhang, W. Long, and L. Geng, Prog. Part. Nucl. Phys. **57**, 470 (2006)
2. P. Ring, Prog. Part. Nucl. Phys. **37**, 193 (1996)
3. J. N. Ginocchio, Phys. Rep. **414**, 165 (2005)
4. J. Meng, K. Sugawara-Tanabe, S. Yamaji, and A. Arima, Phys. Rev. C **59**, 154 (1999)
5. J. Meng, K. Sugawara-Tanabe, S. Yamaji, P. Ring, and A. Arima, Phys. Rev. C **58**, R628 (1998)
6. H. Liang, P. Zhao, Y. Zhang, J. Meng, and N. V. Giai, Phys. Rev. C **83**, 041301 (2011)
7. S. G. Zhou, J. Meng, and P. Ring, Phys. Rev. Lett. **91**, 262501 (2003)
8. W. Koepf and P. Ring, Nucl. Phys. A **493**, 61 (1989)
9. A. V. Afanasjev, P. Ring, and J. König, Nucl. Phys. A **676**, 196 (2000)
10. P. W. Zhao, J. Peng, H. Z. Liang, P. Ring, and J. Meng, Phys. Rev. C **85**, 054310 (2012)

11. P. W. Zhao, J. Peng, H. Z. Liang, P. Ring, and J. Meng, Phys. Rev. Lett. **107**, 122501 (2011)
12. P. W. Zhao, S. Q. Zhang, J. Peng, H. Z. Liang, P. Ring, and J. Meng, Phys. Lett. B **699**, 181 (2011)
13. P. W. Zhao, Z. P. Li, J. M. Yao, and J. Meng, Phys. Rev. C **82**, 054319 (2010)
14. H. Liang, P. Zhao, L. Li, and J. Meng, Phys. Rev. C **83**, 011302 (2011)
15. S. G. Zhou, J. Meng, P. Ring, and E. G. Zhao, Phys. Rev. C **82**, 011301(R) (2010)
16. Z. M. Niu *et al.*, in preparation
17. T. Nikšić, D. Vretenar, and P. Ring, Phys. Rev. C **78**, 034318 (2008)
18. T. Bürvenich, D. G. Madland, J. A. Maruhn, and P. G. Reinhard, Phys. Rev. C **65**, 044308 (2002)
19. G. Audi, A. H. Wapstra, and C. Thibault, Nucl. Phys. A **729**, 337 (2003)
20. M. Girod and B. Grammaticos, Nucl. Phys. A **330**, 40 (1979)
21. S. Raman, C. Nestor, and P. Tikkanen, At. Data Nucl. Data Tables **78**, 1 (2001)
22. J. P. Blaizot, Phys. Rep. **64**, 171 (1980)
23. T. Li *et al.*, Phys. Rev. Lett. **99**, 162503 (2007)
24. H. Sagawa, S. Yoshida, G. M. Zeng, J. Z. Gu, and X. Z. Zhang, Phys. Rev. C **76**, 034327 (2007)
25. K. L. Jones *et al.*, Nature **465**, 454 (2010)
26. G. Lalazissis, S. Karatzikos, R. Fossion, D. P. Arteaga, A. Afanasjev, and P. Ring, Phys. Lett. B **671**, 36 (2009)
27. G. A. Lalazissis, T. Nikšić, D. Vretenar, and P. Ring, Phys. Rev. C **71**, 024312 (2005)
28. W. Long, J. Meng, N. Van Giai, and S. G. Zhou, Phys. Rev. C **69**, 034319 (2004)
29. J. Dobaczewski, H. Flocard, and J. Treiner, Nucl. Phys. A **422**, 103 (1984)
30. J. Bartel, P. Quentin, M. Brack, C. Guet, and H. B. Hakansson, Nucl. Phys. A **386**, 79 (1982)
31. S. Goriely, N. Chamel, and J. M. Pearson, Phys. Rev. Lett. **102**, 152503 (2009)
32. E. Chabanat, P. Bonche, P. Haensel, J. Meyer, and R. Schaeffer, Nucl. Phys. A **635**, 231 (1998)
33. M. Beiner, H. Flocard, N. Van Giai, and P. Quentin, Nucl. Phys. A **238**, 29 (1975)
34. J. Meng, Phys. Rev. C **57**, 1229 (1998)
35. J. Dobaczewski, W. Nazarewicz, T. Werner, J. Berger, C. Chinn, and J. Dechargé, Phys. Rev. C **53**, 2809 (1996)
36. J. Meng and P. Ring, Phys. Rev. Lett. **77**, 3963 (1996)
37. W. Pöschl, D. Vretenar, G. Lalazissis, and P. Ring, Phys. Rev. Lett. **79**, 3841 (1997)
38. G. Lalazissis, D. Vretenar, W. Poschl, and P. Ring, Phys. Lett. B **418**, 7 (1998)
39. J. Meng and P. Ring, Phys. Rev. Lett. **80**, 460 (1998)
40. J. Meng, Nucl. Phys. A **635**, 3 (1998)
41. J. Meng, H. Toki, J. Y. Zeng, S. Q. Zhang, and S. G. Zhou, Phys. Rev. C **65**, 041302 (2002)
42. S. Q. Zhang, J. Meng, and S. G. Zhou, Sci. China G **46**, 632 (2003)
43. J. Meng, I. Tanihata, and S. Yamaji, Phys. Lett. B **419**, 1 (1998)
44. S. G. Zhou, J. Meng, and P. Ring, Phys. Rev. C **68**, 034323 (2003)
45. S. G. Zhou, J. Meng, and P. Ring, AIP Conf. Proc. **865**, 90 (2006)
46. S. G. Zhou, J. Meng, P. Ring, in *Physics of Unstable Nuclei*, edited by D. T. Khoa, P. Egelhof, S. Gales, N. Van Giai, T. Motobayashi (World Scientific, 2008), pp. 402–408 (proceedings of the International Symposium on Physics of Unstable Nuclei, July 3-7, 2007, Hoi An, Vietnam)
47. L. Li, J. Meng, P. Ring, E. Zhao, and S. Zhou, Phys. Rev. C **85**, 024312 (2012)
48. L. L. Li, J. Meng, P. Ring, E. G. Zhao, and S. G. Zhou, Chin. Phys. Lett. **29**, 042101 (2012)
49. Y. Chen, L. Li, H. Liang, and J. Meng, Phys. Rev. C **85**, 067301 (2012)
50. G. A. Lalazissis, J. König, and P. Ring, Phys. Rev. C **55**, 540 (1997)
51. P. Ring and P. Schuck, *The nuclear many-body problem* (Springer-Verlag, New York, 1980)
52. L. L. Li *et al.*, in preparation
53. P. T. Hosmer *et al.*, Phys. Rev. Lett. **94**, 112501 (2005)
54. J. Pereira *et al.*, Phys. Rev. C **79**, 035806 (2009)
55. S. Nishimura *et al.*, Phys. Rev. Lett. **106**, 052502 (2011)
56. N. Paar, T. Nikšić, D. Vretenar, and P. Ring, Phys. Rev. C **69**, 054303 (2004)
57. T. Nikšić, T. Marketin, D. Vretenar, N. Paar, and P. Ring, Phys. Rev. C **71**, 014308 (2005)
58. T. Marketin, D. Vretenar, and P. Ring, Phys. Rev. C **75**, 024304 (2007)